

Article

# Multiple-Embedded-System Optimization Layout for Electromagnetic Wave Power Density in Complex Environments

Yang-Hsin Fan 

Department of Computer Science and Information Engineering, National Taitung University, Taitung 95092, Taiwan; yhfan@nttu.edu.tw; Tel.: +886-89-517-605

Received: 16 July 2020; Accepted: 9 September 2020; Published: 12 September 2020



**Abstract:** Many embedded systems are implemented for healthcare, and smart homes and spaces. These devices are generally designed for elderly care, for monitoring, surveillance, and collection information. As embedded systems are ubiquitous and pervasive in a smart home, office, or space, different layout affects not only reduce the implementation cost but also the power density of electromagnetic waves. This study aimed to develop a multiple-embedded-system optimization layout to consume less electromagnetic wave power density and gain better communication strength. For smart offices, we analyzed the layout topology of  $n$ -shaped and  $n$ -shaped with door layout categories. On the basis of the location of each embedded system in a communication center via an  $n$ -shaped layout, we investigated the electromagnetic wave effect to the local, direct, and semidirect effects. Indirect and subindirect effects were also studied in the  $n$ -shaped layout with a door. In addition, we derived a set of formulas from the scope for the diverse effects to help users to quickly identify the scope of each effect. To verify the multiple-embedded-system optimization layout, 16 cooperating embedded systems with four test cases in a smart office were used to evaluate the diverse effects of electromagnetic wave power density and communication strength. Experiment results showed that the optimization layout consumed  $3950 \times 10^{-6} \text{ W/m}^2$  electromagnetic wave power density.

**Keywords:** embedded system; optimization layout; electromagnetic wave power density

## 1. Introduction

An embedded system is a unique, specific, and highly customized computer system. It consists of a microcontroller and a few input/output devices. Inside the microcontroller are the central processing unit (CPU), program and data memory, and input/output peripheral components. Those components provide simple architectures for a program to execute unique and specific tasks. Additionally, an embedded system has the characteristics of high reliability, less power consumption, easier implementation, being lightweight, and lower cost. Simple architectures with many characteristics attract developers to develop diverse applications for consumer electronics, communication and control industry, and smart appliances.

Simple architectures and characteristics, and diverse peripherals and input/output devices, create various embedded systems such as for temperature, humidity, or light control. Frequently used peripherals have a universal asynchronous receiver/transmitter (UART), serial peripheral interface (SPI), interintegrated circuit (I2C), or secure digital-input/-output (SDIO) interface. They can be used to develop infrared-distance photoelectric data collection, collision-event avoidance, light on/off control, or object-tracking devices [1]. Each embedded system combines one, two, or more peripherals into its design, corresponding to the design specifications. One real-life embedded system is presented

in [2] that comprises a processor, memory, touch screen, display, and UART. It is an embedded e-book system with ARM9 CPU, 32 MB flash memory, a 3.5-inch touch screen, and audio UART. It reduced the design size and cost to smaller and cheaper than those of a personal computer. That is, each component in an embedded system is necessary while tasks are being executed. Consequently, one embedded system does not have any redundant components unless the function of a component is integrated into a microcontroller.

Figure 1 shows diverse embedded systems with various peripherals to connect to miscellaneous sensors. One embedded system is demonstrated in Figure 1a that consists of a microcontroller with UART and I2C peripherals. The UART peripheral is generally used to implement RS-232 to connect two devices. It limits scalability due to merely connecting two devices. If an embedded system needs to connect more devices, a solution is adopting the I2C peripheral. Another embedded system is presented in Figure 1b that comprises a microcontroller, and UART and SPI peripherals. The SPI interface is faster than I2C is. Another embedded system is illustrated in Figure 1c that is composed of a microcontroller, UART, SPI, and SDIO. The SDIO interface can not only connect more devices. It also extends communication by wired or wireless protocols. Figure 2 shows four applications adopting the aforementioned embedded systems in a smart home, office, or space.

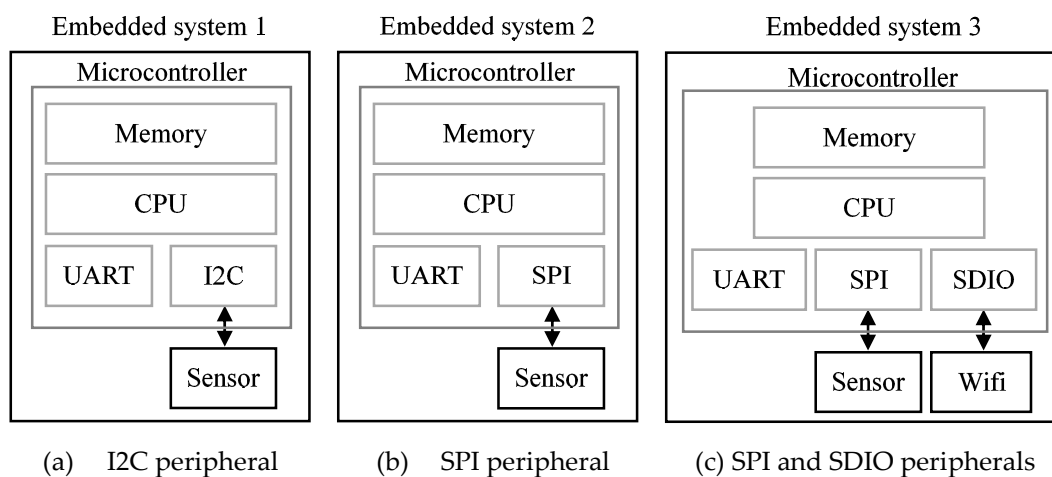


**Figure 1.** Diverse peripherals for embedded systems. Note: I2C, interintegrated circuit; SPI, serial peripheral interface; SDIO, secure digital-input/-output interface.

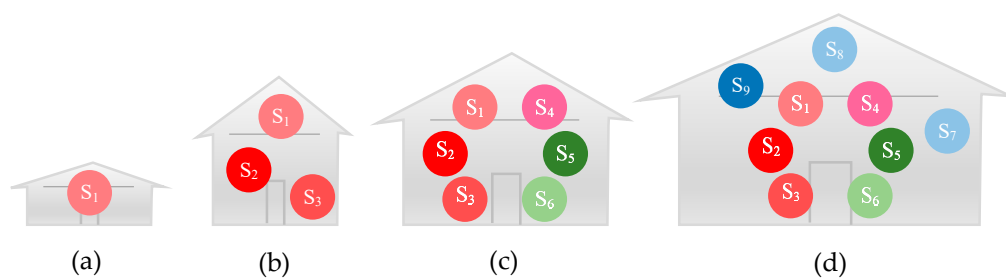


**Figure 2.** Embedded-system layout applications. (a) One, (b) three, (c) six, and (d) nine embedded systems.

There is a rising number of embedded systems that integrate sensors to work in a smart home. According to sensor market trends, it is expected that a massive number of sensors will be deployed in future households. Therefore, Klemenjak and Elmenreich [3] aimed to analyze user behavior and energy consumption. They presented an open-hardware energy measurement approach to reflect the power consumption of a certain appliance and impact on the environment. Visutsak and Daoudi [4] addressed smart home technology for the elderly, and proposed a specific smart home model with a selection of passive and active-intervention devices. In order for devices to communicate with

each other, the Internet of Things is usually adopted as the network technology. Florea et al. [5] addressed several standardized protocols with diverse networking levels on embedded devices to achieve low memory, processing power, and data rate. Chen et al. [6] also applied the Internet of Things to interconnect and have embedded systems and smart devices to collaborate in cyber-physical systems. In the smart-sensory-furniture (SSF) project of ambient assisted living, Bleda et al. [7] presented an SSF sensor layer for sensing massively distributed objects with energy limitations and other factors. Researchers such as Chen et al. [6], and Bleda et al. [7] expressed a need to process the awareness information from pervasive sensors because they adopted Internet of Things technology. Lalanda et al. [8] defined a self-aware solution relationship mechanism and proposed context-management software in a service-oriented pervasive environment. As opposed to software, Adiono et al. [9] presented prototyping for controlling devices in smart homes. Considering the shift from the smart home to an overall smart space, issues relating to interconnectedness, collaboration, monitoring, management, control, or power consumption have become more complex. Zeng et al. [10] proposed a system-level design approach for smart spaces that constrained cost and power consumption. Regarding it as a multiobjective issue, Deuri and Sathya [11] proposed the cricket-chirping algorithm, and validated their solution using multiobjective test functions. It was used to solve the disc brake and weld beam design problems. As a problem from multiple object functions evolves to multiple levels, Dutta and Datta [12] applied a combine-and-transform method to combine both levels of a multiobjective optimization problem to a single level. Zhou [13] presented a decomposition-based multiobjective tabu search algorithm for multiobjective unconstrained binary quadratic programming problems. The procedures included uniform weight-vector collection decomposed into an aggregation function set and tabu search. Experiment results showed that the proposed solution was effective in meeting its benchmarks.

## 2. Problem Formulation

A smart office usually splits spaces into business, work, or meeting room areas. A smart home has a few spaces, such as the living room, kitchen, bedroom, and dining room. These spaces generally have some embedded systems set up for collecting data, detecting smoke, or tracking objects for office protection or home care. From an architecture viewpoint, those embedded systems form distributed embedded systems with wireless services in different spaces to the communication center for transferring data. However, interfering substances such as walls, doors, furniture, beam columns, and electromagnetic radiation implicitly or explicitly affect communication strength between embedded systems and the communication center, resulting in each embedded system needing more electromagnetic wave power density for data transfer. Consequently, locations in different spaces of distributed embedded systems and the communication center, called the embedded system layout, require a good arrangement for better electromagnetic signal strength and less electromagnetic wave energy consumption. Moreover, in focusing on an embedded system layout, we assumed the following. First, due to electromagnetic radiation, electromagnetic wave power density through walls is classified into semidirect, indirect, or/and subindirect effects. Second, wall reflection and absorption were ignored because they are hard to identify. Third, electromagnetic wave power density was generated by the communication center and embedded systems. Lastly, the measured electromagnetic wave power density included the transmitter and received data.

## 3. Multiple-Embedded-System Optimization Layout

### 3.1. Initial Measurement for Electromagnetic Wave Power Density

This work studies the embedded system-layout approach for better electromagnetic signal strength and less electromagnetic wave power density at smart offices. Figure 3 demonstrates an example of a multiple-embedded-system layout at a smart office with business, work, and meeting room areas for an indoor floor plane. Each embedded system was named  $S_0, S_1, \dots$ , and  $S_{15}$ , respectively. The location

and distance layout considered electromagnetic wave strength and power density. Electromagnetic waves are ubiquitous and they propagate energy through space. Two expressions, -dBm and power density, are frequently used to assess the electromagnetic wave effect.

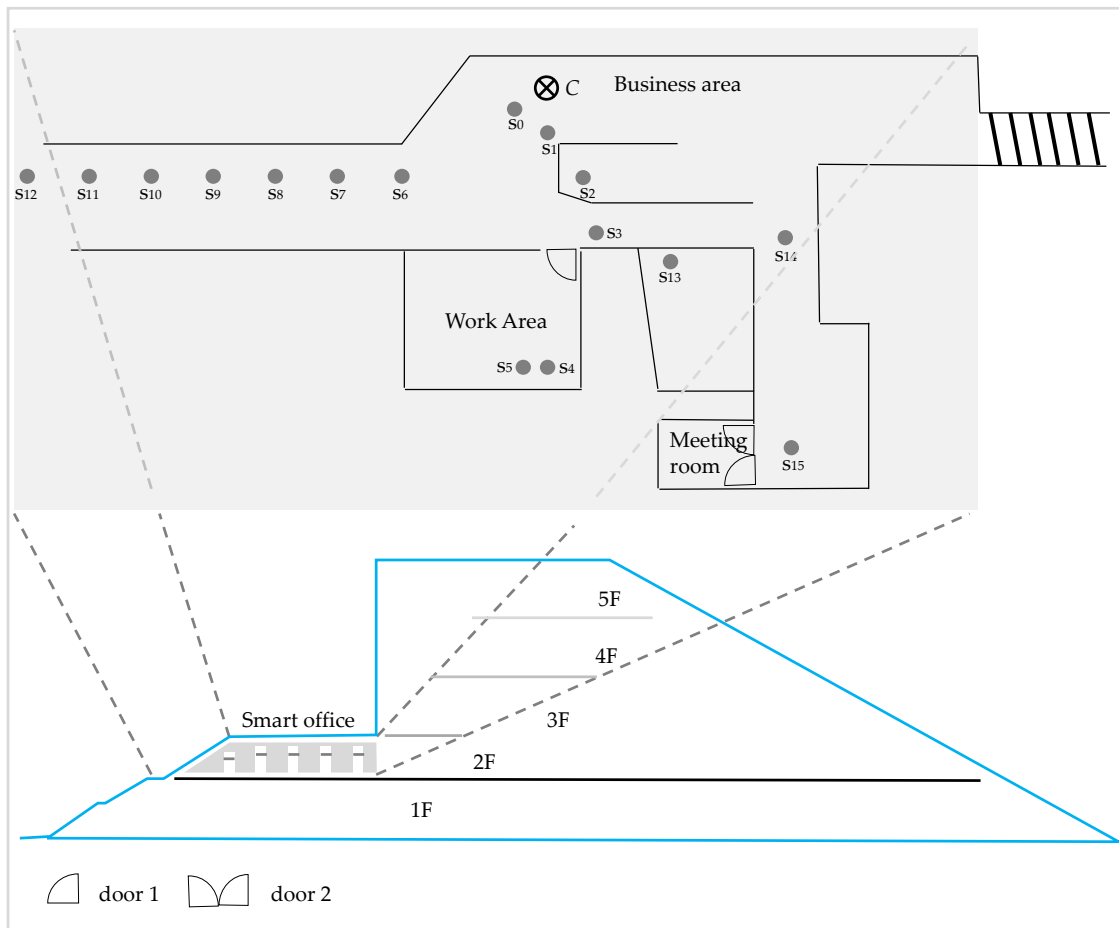


**Figure 3.** Multiple-embedded-system layout at smart office for indoor floor plane.

The former is used to define electromagnetic signal strength in the microwave (MW) or radio-frequency (RF) field. It is generally represented as negative. The range from 0 to 80-dBm represents electromagnetic wave strength. Being nearer to zero indicates better electromagnetic strength. The latter is used to evaluate the power consumption per transmitter area between source and receiver.

Electromagnetic waves are ubiquitous in any environment. In order to investigate the original data of electromagnetic signal strength and power density, shown in Figure 3, we measured electromagnetic wave strength and power consumption per area at  $S_0, S_1, \dots, S_{15}$  with a Wi-Fi analyzer [14], multiple-route optimization layout (MROL) applications, and a Tenmars TM-196 instrument [15]. We measured 16 different locations for two reasons: (a) each location was a candidate for setting up an embedded system, and (b) to analyze the effect of locations and distances for various layouts. On the one hand, the Wi-Fi analyzer, downloaded for free from the Google app store, could be used to detect the electromagnetic wave strength of a wireless access point in space. On the other hand, we developed the multiple-route optimization layout (MROL) application to obtain a better layout with better electromagnetic signal strength and less electromagnetic power density of embedded systems. Both applications were executed in an Android operating system of a mobile platform. Table 1 shows the results of the original data from Figure 3. The Location column represents the site of embedded systems. The Dist. column represents the distance between the communication center and embedded

system. The -dBm column indicates the electromagnetic signal strength, and the Power Density column shows power consumption per area. Figure 4 shows the original data of electromagnetic wave power density for  $S_0, S_1, \dots$ , and  $S_{15}$ .

**Table 1.** Original data of signal strength and total electromagnetic wave power density for  $S_0, S_1, \dots$ , and  $S_{15}$ . Note: MROL, multiple-route optimization layout.

		Wi-Fi Analyzer			MROL			Wi-Fi Analyzer			MROL			
Location	Dist.	-dBm	-dBm	Power Density	Location	Dist.	-dBm	-dBm	Power Density	Location	Dist.	-dBm	-dBm	Power Density
	m			( $10^{-6} \text{ W/m}^2$ )		m			( $10^{-6} \text{ W/m}^2$ )		m			( $10^{-6} \text{ W/m}^2$ )
$S_0$	0	78	80	55	$S_8$	9.28	84	87	35	$S_8$	9.28	84	87	35
$S_1$	1	79	79	70	$S_9$	13.28	87	85	21	$S_9$	13.28	87	85	21
$S_2$	5	79	80	50	$S_{10}$	17.28	83	81	30	$S_{10}$	17.28	83	81	30
$S_3$	10	87	83	40	$S_{11}$	21.28	83	81	35	$S_{11}$	21.28	83	81	35
$S_4$	15	95	94	95	$S_{12}$	25.28	92	88	100	$S_{12}$	25.28	92	88	100
$S_5$	15.03	96	94	120	$S_{13}$	15.5	86	89	20	$S_{13}$	15.5	86	89	20
$S_6$	4	76	78	70	$S_{14}$	22	87	88	20	$S_{14}$	22	87	88	20
$S_7$	5.66	77	79	20	$S_{15}$	26	94	94	60	$S_{15}$	26	94	94	60
Minor total		667	667	520	Minor total		696	693	321	Minor total		696	693	321
Total					Total		1363	1360	841	Total		1363	1360	841

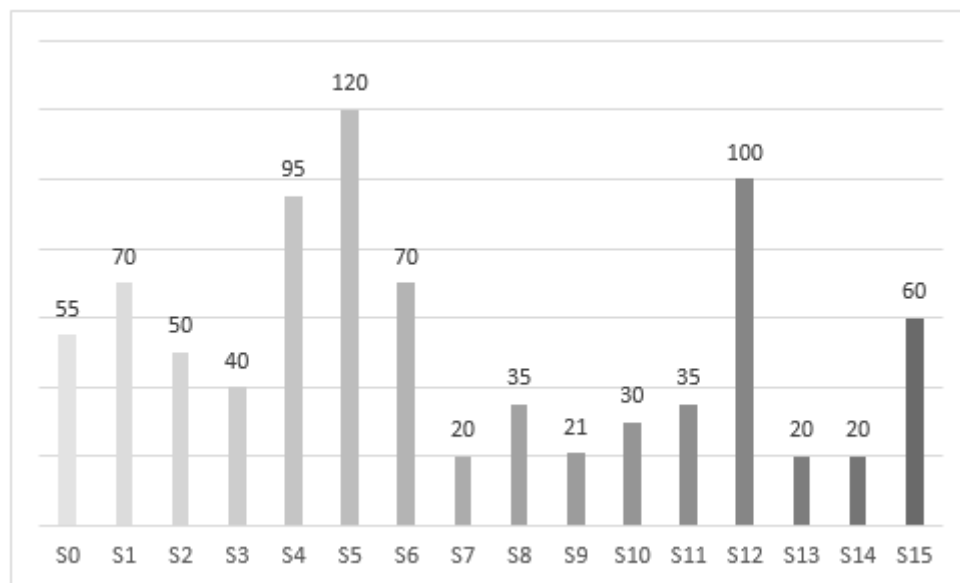


**Figure 4.** Original data of electromagnetic wave power density for  $S_0, S_1, \dots$ , and  $S_{15}$ .

### 3.2. Layout Topology

According to the results in Table 1, the location and distance layout affects -dBm and electromagnetic wave power density. Figure 5 demonstrates layout examples with many embedded systems, a communication center, and obstacles. Sign 0 in Figure 5a represents a communication center providing a wireless network service for all embedded systems. Sign 1 represents an embedded system that works for detecting, monitoring, or collecting data. In reality, location, distance, and also doors and walls may interfere with or block the communication path between Signs 0 and 1. The white square under the graph represents interference factors between Signs 0 and 1 such as air, temperature, humidity, and obstacles. While an embedded system transfers data through white squares via a green path, it may consume more power density than the red path does. Otherwise, to rearrange the layout of the communication center with a dotted line, and to a route with a red gain, less power consumption per area and better communication strength among embedded systems are needed. Rearranging a

layout results in changes in the locations, distances, and obstacle paths between the communication center and embedded systems. Either-dBm or power density is affected. As an increasing number of embedded systems are deployed into smart homes or offices, the layout becomes more complex for locations, distances, and obstacles between the communication center and embedded systems. For example, Figure 5b–d illustrates the layout topology for three, six, and nine embedded systems in smart homes, offices, or other complex environments. Each layout shows two kinds of topologies in red and green. In fact, there are various layout topologies for each space. One can have multiobjective optimization with obstacles, better electromagnetic wave strength, and less electromagnetic effect.

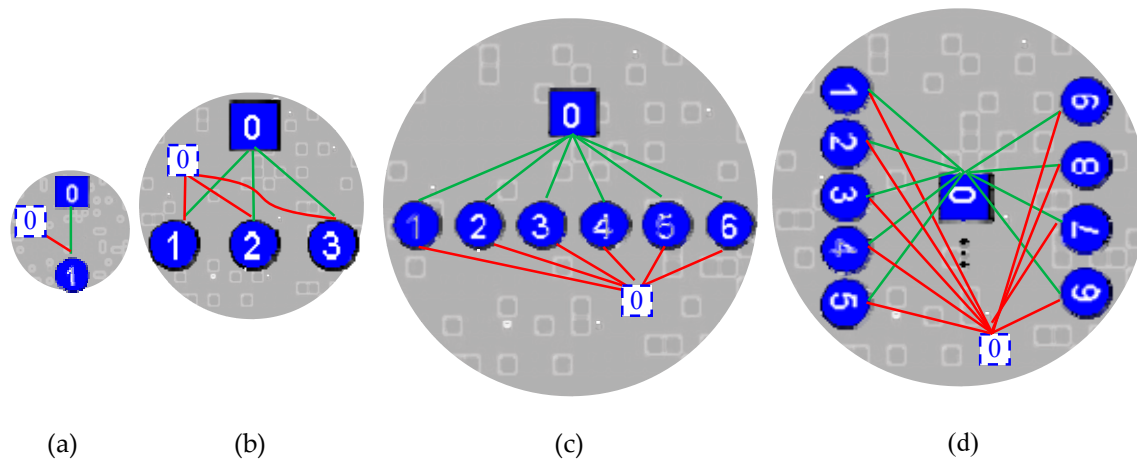


Figure 5. Distributed embedded system deployment in a complex environment.

### 3.3. *n*-Shaped Layout

Figure 3 shows a business area where some embedded systems were set up. The business area had three side walls, as shown in Figure 6, which we called an *n*-shaped layout. In practice, most designers set the location of a communication center at the center or near-center of an *n*-shaped space as shown in Figure 6a–c. For such a space, we analyzed the effect factors of electromagnetic waves as  $l_1$ ,  $l_2$ ,  $R$ ,  $r_1$ ,  $r_2$ ,  $L$ , and  $W$ , which are depicted in Figure 7. For Figure 7a,  $l_1$  and  $l_2$  represent the length from the communication center to the edge of the left and the right side, respectively.  $R$  is the circle radius for electromagnetic waves.  $r_1$  and  $r_2$  are the lengths from the edge of the left and the right side, respectively, to the circumference.  $L$  and  $W$  are the length and width for the *n*-shaped layout, respectively. There were also five limitations. One was the floor that was limited in the same plane because the smart office only had two floors in this study. That is, either the upper or the lower floor did not need to be considered. Another limitation regards the entrance. Both the left and right walls of the *n*-shaped layout had an entrance to set up embedded systems, shown with a red circle. The front wall was not a way in or out, shown by the grid symbol. The other limitations were  $l_1 < W$ ,  $l_2 < W$ , and  $l_1 = l_2$  because the communication center was set at the center or near-center. Either  $l_1$  or  $l_2$  was variant, and they were the values corresponding to the location of the communication center.

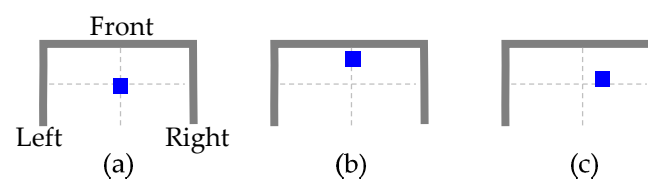
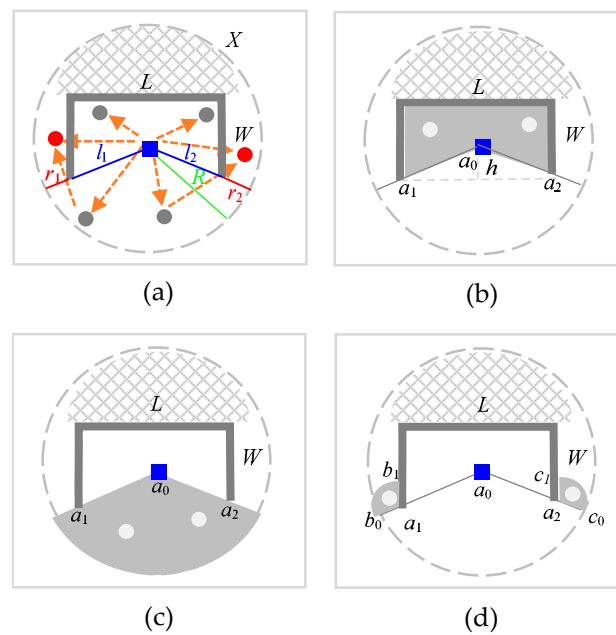


Figure 6. Locations of the communication center in an *n*-shaped layout.



**Figure 7.** *n*-shaped layout. (a) Radiation of power density distribution. (b) Local, (c) direct, and (d) semidirect effects.

Figure 7a presents a six-embedded-system layout in an *n*-shaped space. According to the results of the original data measurement in Table 1, we categorized electromagnetic signal strength and power density distribution into local, direct, and semidirect effects, shown in Figure 7b–d, respectively. First, the local effect is shown in Figure 7b, and it has three characteristics. (a) The embedded systems and communication center were located inside the *n* shape. Therefore, each embedded system could communicate with the communication center inside the *n* shape. (b) It was without obstacles between the communication center and embedded systems, obtaining better electromagnetic signal strength. (c) This regarded the electromagnetic signal coverage that was dependent on radiation angle  $a_0$  between embedded systems and the communication center. On the basis of the aforementioned characteristics, embedded systems in a local effect could gain the best electromagnetic signal and the least electromagnetic wave power density. The scope of the local effect can be seen in formula form below:

$$\left( L \times W - \frac{L \times h}{2} \right) \tag{1}$$

where  $h$  represents the height of triangle  $a_1a_0a_2$ .

Electromagnetic wave power density for embedded systems in a local effect can be evaluated with the sum of the number of embedded systems as follows:

$$\sum_i S_i \tag{2}$$

where  $i$  represents the number of embedded systems.

Second, the direct effect that is illustrated in Figure 7c has three characteristics: (a) The location of the embedded systems. Embedded systems can directly transmit electromagnetic signals to the communication center because their locations have better electromagnetic signal strength. (b) It is without obstacles between the communication center and embedded systems. These two features are the same as those of the local effect, but the difference is in terms of location and distance. (c) The electromagnetic signal coverage is determined by the radiation angle from  $a_0$  to  $a_2$ . As shown in Figure 7c, the area shape of the direct effect can be seen in formula form as follows:

$$(R^2\pi \times \frac{\angle a_1 a_0 a_2}{360^\circ}) \quad (3)$$

where  $R$  represents the radius of circle  $X$ .

Additionally, electromagnetic wave power density for embedded systems can be evaluated with the sum of the number of embedded systems as follows:

$$\sum_j S_j \quad (4)$$

where  $j$  represents the number of embedded systems in direct effect.

Third, the semidirect effect is displayed in Figure 7d, which is the specific location in the neighborhood of  $r_1$  and  $r_2$ , respectively. It is called semidirect because the electromagnetic signal is interfered with by wall obstacles. In addition, the effect source may originate from either a local or a direct effect. Consequently, the area of the semidirect effect consisted of two scopes, as follows:

$$(R - l_1)^2\pi \times \frac{\angle b_0 a_1 b_1}{360^\circ} \quad (5)$$

$$(R - l_2)^2\pi \times \frac{\angle c_0 a_2 c_1}{360^\circ} \quad (6)$$

where  $b_0 a_1 b_1$  and  $c_0 a_2 c_1$  represent the left and right sector, respectively. In addition, the electromagnetic wave power density of embedded systems can be evaluated with the sum of the number of embedded systems as follows:

$$\sum_k S_k \quad (7)$$

where  $k$  represents the number of embedded systems in semidirect effect.

In summary, the optimization power density of the electromagnetic waves of embedded systems for an  $n$ -shaped layout is calculated using

$$\text{Min}P(i, j, k) = \sum_i S_i + \sum_j S_j + \sum_k S_k \quad (8)$$

### 3.4. $n$ Shape with Door Layout

Except for needing to discuss the  $n$ -shaped space, another  $n$ -shaped space with a door is frequently seen in smart homes or offices. Figure 8 exhibits five kinds of  $n$ -shaped layouts with a door. Figure 8a–c demonstrates three kinds of  $n$ -shaped communication center layouts with a wider door. Figure 8d,e displays two kinds of communication center layouts in an  $n$  shape with a narrower door. We analyzed the effect factors for  $n$ -shaped layouts with a wider and narrower door, shown in Figure 9. Those effect parameters consisted of  $l_1$ ,  $l_2$ ,  $R$ ,  $d_1$ ,  $d_2$ ,  $L$ , and  $W$ , depicted in Figure 9a.  $l_1$  and  $l_2$  are the lengths from the center of a circle to the edge of the left and right sides, respectively.  $R$  is the radius of the circle for electromagnetic waves.  $d_1$  and  $d_2$  represent the length of the left and right door, respectively.  $L$  and  $W$  are the length and width, respectively. There were also four limitations. The first is the same as that of the  $n$ -shaped layout that was addressed in Section 3.3. Second, it had an entrance to set up embedded systems behind the front wall. Third, either a wider or a narrower door was in the way of obstacles that could interfere with -dBm and power density. The fourth limitation was the communication center being set at the center or near-center.

Figure 9a presents an  $n$ -shaped eight-embedded-system layout with a door space. We categorized electromagnetic signal strength and power density distribution into local, direct, semidirect, indirect, and subindirect effects. Figure 9b displays the local effect, whose characteristics were the same as those of the local effect of the  $n$ -shaped layout that was addressed in Section 3.3. According to Figure 9b, the scope of the local effect can be formulated as follows:

$$L \times W - \frac{[L - (d_1 + d_2)] \times h}{2} \quad (9)$$

where  $h$  represents the triangle height. In addition, electromagnetic wave power density for embedded systems could be evaluated with the sum of the number of embedded systems as follows:

$$\sum_i S_i \quad (10)$$

where  $i$  represents the number of embedded systems.

Figure 9c demonstrates the direct effect with the same characteristics as those of the direct effect of the  $n$ -shaped layout. The scope is in formula form below.

$$R^2 \pi \times \frac{\angle a_1 a_0 a_2}{360^\circ} \quad (11)$$

where  $R$  represents the radius of circle  $X$ . In addition, electromagnetic wave power density for embedded systems can be evaluated with the sum of the number of embedded systems as follows.

$$\sum_j S_j \quad (12)$$

where  $j$  represents the number of embedded systems in direct effect.

Figure 9d demonstrates the semidirect effect that was located in the neighborhood of the direct effect. It consisted of the left and right sectors, respectively. Therefore, the scope could be formulated as follows:

$$\left\{ [(R - l_1)^2 \pi \times \frac{\angle b_{01} b_{00} b_{02}}{360^\circ}] \right\} + \left\{ [(R - l_2)^2 \pi \times \frac{\angle b_{11} b_{10} b_{12}}{360^\circ}] \right\} \quad (13)$$

where  $b_{01} b_{00} b_{02}$  and  $b_{11} b_{10} b_{12}$  represent the left and right sectors, respectively. If  $d_1 = d_2$  and  $l_1 = l_2$ , the scope can be formulated as follows:

$$\left\{ [(R - l_1)^2 \pi \times \frac{\angle b_{01} b_{00} b_{02}}{360^\circ}] \right\} \times 2 \quad (14)$$

In addition, electromagnetic wave power density for embedded systems can be evaluated with the sum of the number of embedded systems as follows:

$$\sum_k S_k \quad (15)$$

where  $k$  represents the number of embedded systems in semidirect effect.

Figure 9e demonstrates the indirect effect that was located in the neighborhood of the local effect. It consisted of the left and right sectors, respectively. Therefore, the scope could be formulated as follows:

$$\left\{ [(R - l_1 - d_1)^2 \pi \times \frac{\angle c_{01} c_{00} c_{02}}{360^\circ}] \right\} + \left\{ [(R - l_2 - d_2)^2 \pi \times \frac{\angle c_{11} c_{10} c_{12}}{360^\circ}] \right\} \quad (16)$$

where  $c_{01} c_{00} c_{02}$  and  $c_{11} c_{10} c_{12}$  represent the left and right sector, respectively. If  $d_1 = d_2$  and  $l_1 = l_2$ , the scope is as follows:

$$\left\{ [(R - l_1 - d_1)^2 \pi \times \frac{\angle c_{01} c_{00} c_{02}}{360^\circ}] \right\} \times 2 \quad (17)$$

In addition, electromagnetic wave power density for embedded systems can be evaluated with the sum of the number of embedded systems as follows:

$$\sum_m S_m \quad (18)$$

where  $m$  represents the number of embedded systems in indirect effect.

Figure 9f demonstrates the subindirect effect that was located at  $L$ . It consisted of the left and right sectors, respectively. Therefore, the scope could be formulated as follows:

$$\{[(R - l_1 - d_1 - W)^2\pi \times \frac{\angle e_{01}e_{00}e_{02}}{360^\circ}]\} + \{[(R - l_2 - d_2 - W)^2\pi \times \frac{\angle e_{11}e_{10}e_{12}}{360^\circ}]\} \quad (19)$$

where  $e_{01}e_{00}e_{02}$  and  $e_{11}e_{10}e_{12}$  represent the left and right sector, respectively. If  $d_1 = d_2$  and  $l_1 = l_2$ , the scope could be formulated as follows:

$$\{[(R - l_1 - d_1 - W)^2\pi \times \frac{\angle e_{01}e_{00}e_{02}}{360^\circ}]\} \times 2 \quad (20)$$

In addition, electromagnetic wave power density for embedded systems can be evaluated with the sum of the number of embedded systems as follows:

$$\sum_n S_n \quad (21)$$

where  $n$  represents the number of embedded systems in subindirect effect.

The optimization power density of electromagnetic waves for an  $n$ -shaped layout with a door is calculated with

$$\text{Min}P(i, j, k, m, n) = \sum_i S_i + \sum_j S_j + \sum_k S_k + \sum_m S_m + \sum_n S_n \quad (22)$$

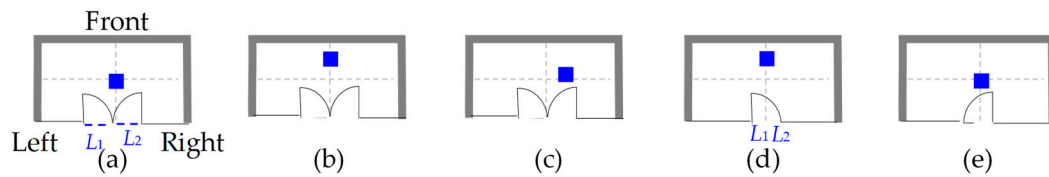


**Figure 8.** Variant locations of the communication center in an  $n$ -shaped layout with a door. (a–c) demonstrates three kinds of  $n$ -shaped communication center layouts with a wider door. (d,e) displays two kinds of communication center layouts in an  $n$  shape with a narrower door.

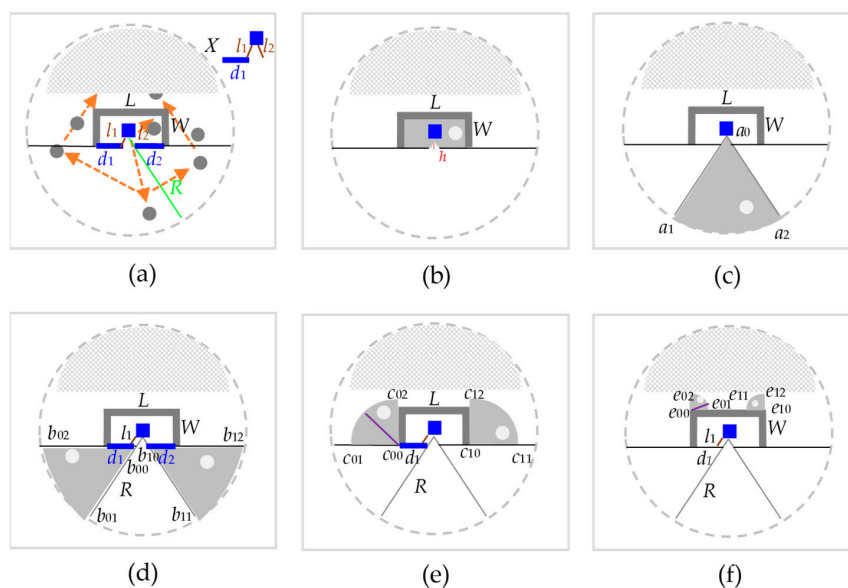


**Figure 9.**  $n$ -shaped layout with a door. (a) Radiation of power density distribution. (b) Local, (c) direct, (d) semidirect, (e) indirect, and (f) subindirect effects.

#### 4. Experiment Results

Figure 3 illustrates the smart office with business, work, and meeting room areas where a communication center  $C$  and 16 embedded systems  $S_0, S_1, \dots$ , and  $S_{15}$  were set up. We implemented embedded systems with a wireless function in an Arduino WeMos D1 miniplatform [16]. The evaluation tools included hardware and software. Hardware was the Tenmars TM-196 instrument [15], Fortinet FortiAP-221C [17], and mobile power bank [18], which were used to measure electromagnetic wave power density, serve wireless service, and supply power for Arduino embedded systems, respectively. We developed MROL application software to detect and assess the communication quality among the communication center and embedded systems.

According to the locations of the 16 kinds of embedded systems in Figure 3, four candidates of the communication center, namely,  $C_1, C_2, C_3$ , and  $C_4$ , were used to assess the proposed multiobjective optimization embedded system layout. Figure 10 exhibits the first test case  $C_1$  at the business area. The measured results of electromagnetic wave power density and signal strength are shown in Figure 11 and Table 2, respectively. The Dist. column represents the Euclidean distance from  $C_1$  to the embedded system. The -dBm column represents the communication strength between  $C_1$  to the embedded system. The P.D. column represents electromagnetic wave power density. The first test case was mainly used to assess the  $n$ -shaped layout effect. For  $S_0$ , it was set at local effect. Consequently, it had the best communication strength, but consumed the highest electromagnetic wave power density. The measured data for communication strength and electromagnetic wave power density in Table 2 were 34-dBm and  $2500 \times 10^{-6} \text{ W/m}^2$ , respectively. The significant value of  $2500 \times 10^{-6} \text{ W/m}^2$  was because the location was the nearest to  $C_1$ .  $S_1, S_2, S_3, S_6$ , and  $S_7$  were located in the direct-effect area. Those embedded systems had better communication strength and electromagnetic wave power density. The measured results were between 39 and 49-dBm for the former, and 30 and  $55 \times 10^{-6} \text{ W/m}^2$  for the latter.  $S_8, S_9$ – $S_{12}$ , and  $S_{14}$  worked in the semidirect-effect area. Communication strength progressively decreased, corresponding to the distance. According to the experiment, communication quality was worse while the communication strength value was greater than 65-dBm. As a result,  $S_{10}$ – $S_{12}$  were the candidates to rearrange the locations.  $S_{12}$  measured electromagnetic wave power density to be  $40 \times 10^{-6} \text{ W/m}^2$ . This was different from  $S_{10}$  or  $S_{11}$ , perhaps because another unknown communication center was located in another building close to  $S_{12}$ . Other embedded systems  $S_4, S_5, S_{13}$ , and  $S_{15}$  were classified into an  $n$ -shaped layout with a door. In order to distinguish the effects from  $n$ -shaped layout, the effect column in Table 2 was labeled in lowercase.  $S_4$  worked in the direct-effect area to gain better communication strength than that of  $S_5$ . However, it had higher electromagnetic wave power density than that of  $S_5$  due to the direct path of the electromagnetic wave through the door.  $S_5$  was located in the semidirect-effect area with weaker communication strength than that of  $S_4$ .  $S_{13}$  was located in the indirect effect area with a communication strength of 60-dBm.  $S_{15}$  was located in the subindirect-effect area with weak communication strength because of a value greater than 65-dBm. Considering electromagnetic wave power density, all embedded systems consumed  $3116 \times 10^{-6} \text{ W/m}^2$ .

The second test case is demonstrated in Figure 12, where  $C_2$  was set as the work area. The measured results of electromagnetic wave power density are demonstrated in Figure 13. This test case was used to evaluate the  $n$ -shaped layout with a door. In order to distinguish the effect from that of the  $n$ -shaped layout, the effect column in Table 2 was labeled in lowercase.  $S_4$  and  $S_5$  were located in the local effect area, resulting in the best communication strength gained, with 33 and 32-dBm, respectively.  $S_5$  consumed the most electromagnetic wave power density,  $7000 \times 10^{-6} \text{ W/m}^2$ , in comparison to other embedded systems due to its location being the nearest to  $C_2$ .  $S_1$  was located in the direct-effect area that had better communication strength than that of  $S_0$ . In comparison, with electromagnetic wave power density to  $S_0, S_1$ , and  $S_0$  consumed 50 and  $100 \times 10^{-6} \text{ W/m}^2$ , respectively.  $S_0, S_2, S_3, S_6, S_7$  to  $S_{12}$ , and  $S_{14}$  were located in the semidirect-effect area with values of communication strength from 57 to 74-dBm. According to the experiment, communication quality was worse while the value of communication strength was greater than 65-dBm. Therefore,  $S_{11}, S_{12}$ , and  $S_{14}$  were the candidates to rearrange the locations.  $S_{13}$  and  $S_{15}$  were located in the subindirect-effect area with worse communication quality,

resulting in them becoming candidates to rearrange the locations. Considering electromagnetic wave power density, all embedded systems consumed  $7800 \times 10^{-6} \text{ W/m}^2$ .

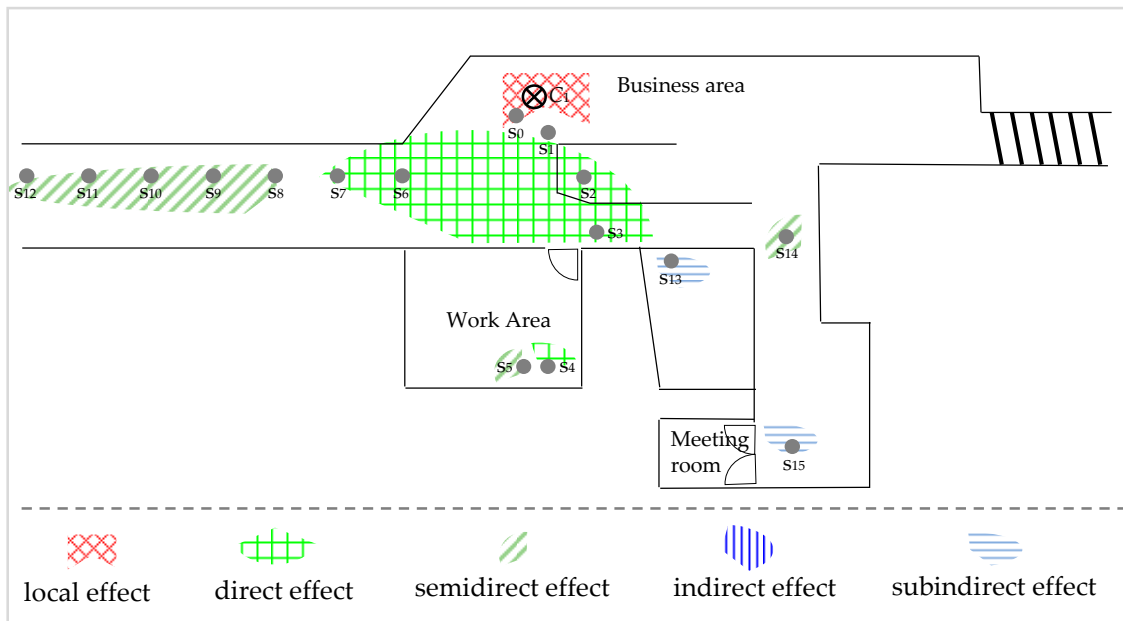


Figure 10. Various effects for  $C_1$  and 16-embedded-system layout.

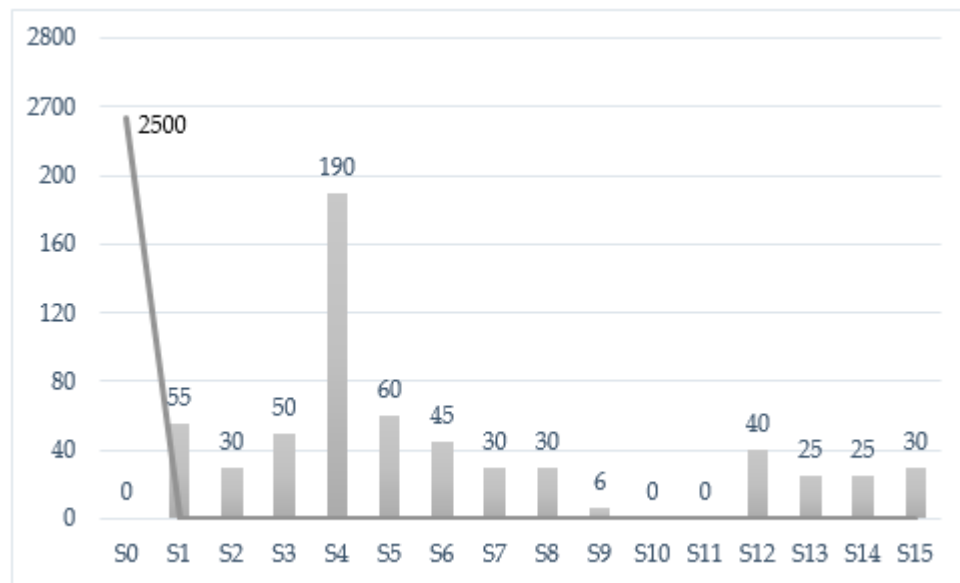


Figure 11. Electromagnetic wave power density for  $C_1$  to  $S_0, S_1, \dots$ , and  $S_{15}$ .

Because the first and second test cases had few candidates for rearrangement, the third and fourth test cases aimed to decrease the number of rearrangement candidates to improve the embedded system layout. Figure 14 shows the third test case that set up  $C_3$  at the  $S_6$  location. Embedded systems except for  $S_4, S_5, S_{13}$ , and  $S_{15}$  are discussed with regard to the  $n$ -shaped layout. From the viewpoint of  $-dBm$  in MROL in Table 3, values from 33 to 56 indicated that those embedded systems had better communication strength. On the other hand, considering  $S_4, S_5, S_{13}$ , and  $S_{15}$  with an  $n$ -shaped layout with a door, only  $S_{15}$  had worse communication quality. Only one embedded system needed rearrangement. Considering electromagnetic wave power density, it consumed  $3950 \times 10^{-6} \text{ W/m}^2$  for all embedded systems; measured results are illustrated in Figure 15. The final test case set  $C_4$  at the  $S_3$  location. Embedded systems except for  $S_4, S_5$ , and  $S_{13}$  are discussed with regard to the  $n$ -shaped

layout. The values of -dBm in MROL ranged from 35 to 73. There were three embedded systems,  $S_{10}$ – $S_{12}$ , with worse communication strength that needed to be rearranged. Embedded systems with an  $n$ -shaped layout with a door had efficient enough communication strength to work.

**Table 2.** Comparison of electromagnetic wave signal strength and total electromagnetic wave power density for  $S_0, S_1, \dots$ , and  $S_{15}$  to  $C_1$  and  $C_2$ .

Test Case 1				$C_1$		Test Case 2				$C_2$	
Wi-Fi Analyzer				MROL		Wi-Fi Analyzer				MROL	
E.S.	Dist.	-dBm	Effect	-dBm	P. D.	E.S.	Dist.	-dBm	Effect	-dBm	P. D.
	m				( $10^{-6} \text{ W/m}^2$ )		m				( $10^{-6} \text{ W/m}^2$ )
$S_0$	0	31	L	34	2500	$S_0$	15.1	65	sd	65	100
$S_1$	1	36	D	39	55	$S_1$	14.4	55	d	55	50
$S_2$	5	45	D	49	30	$S_2$	14.1	66	sd	66	50
$S_3$	10	43	D	41	50	$S_3$	11.4	59	sd	59	50
$S_4$	15	62	d	56	190	$S_4$	1	33	L	33	200
$S_5$	15	56	sd	60	60	$S_5$	0	32	L	32	7000
$S_6$	4	43	D	39	45	$S_6$	11.1	57	sd	57	60
$S_7$	5.7	45	D	45	30	$S_7$	15.1	60	sd	60	50
$S_8$	9.3	54	SD	54	30	$S_8$	19.1	61	sd	61	20
$S_9$	13.3	61	SD	58	6	$S_9$	23.1	63	sd	63	12
$S_{10}$	17.3	70	SD	70	0	$S_{10}$	27.1	65	sd	63	18
$S_{11}$	21.3	73	SD	73	0	$S_{11}$	31.1	73	sd	73	20
$S_{12}$	25.3	76	SD	76	40	$S_{12}$	35.1	74	sd	74	100
$S_{13}$	15.5	51	i.	60	25	$S_{13}$	16.9	67	si	67	30
$S_{14}$	22	70	SD	65	25	$S_{14}$	23.4	67	sd	71	20
$S_{15}$	26	77	si	77	30	$S_{15}$	27.4	79	si	85	20
Total		893		896	3116	Total		976		984	7800

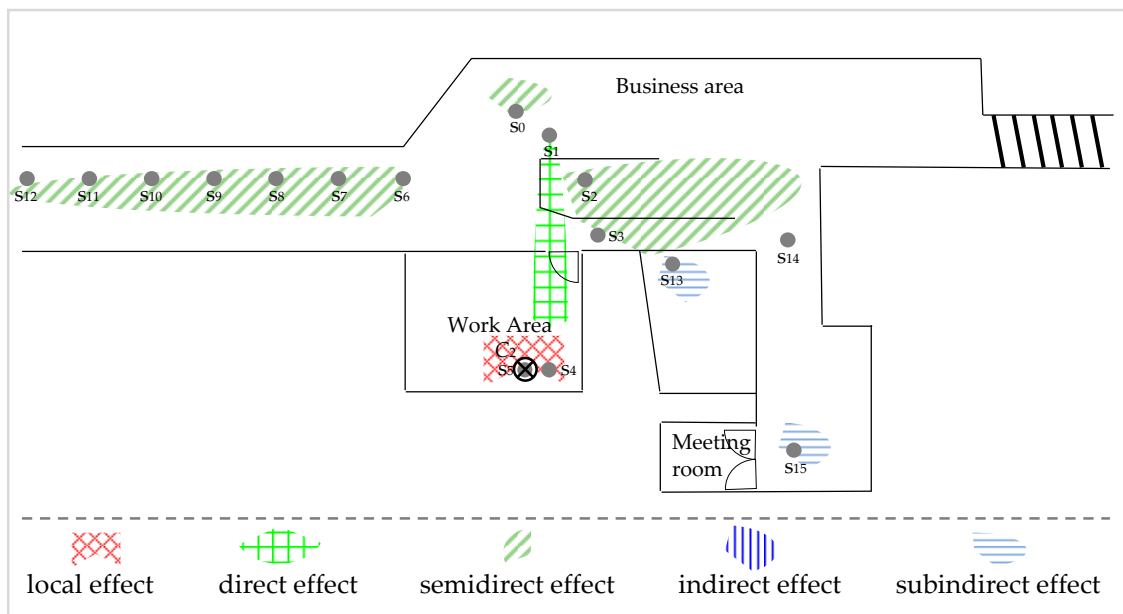


**Figure 12.** Various effects for  $C_2$  and 16 embedded system layouts.

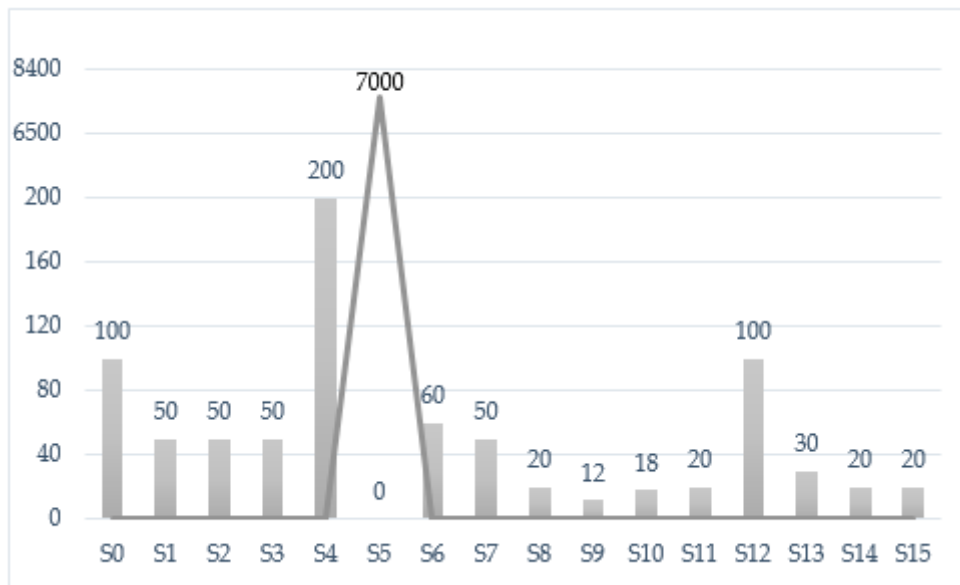


Figure 13. Electromagnetic wave power density for C<sub>2</sub> to S<sub>0</sub>, S<sub>1</sub>, . . . , and S<sub>15</sub>.

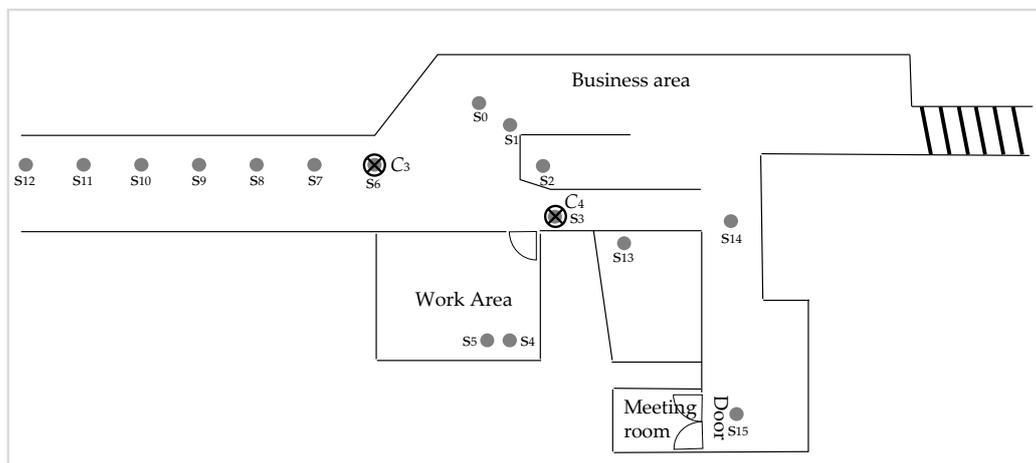


Figure 14. C<sub>3</sub>, C<sub>4</sub> and 16-embedded-system layout.

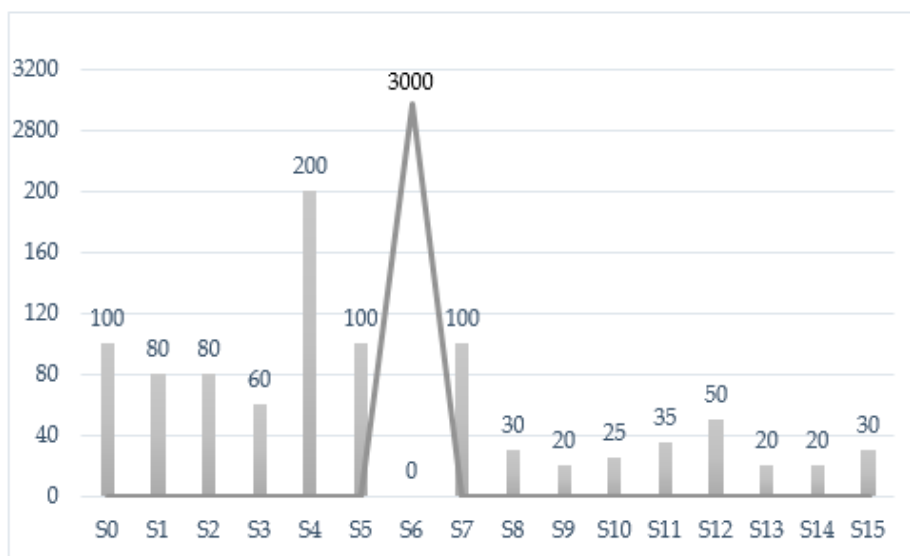
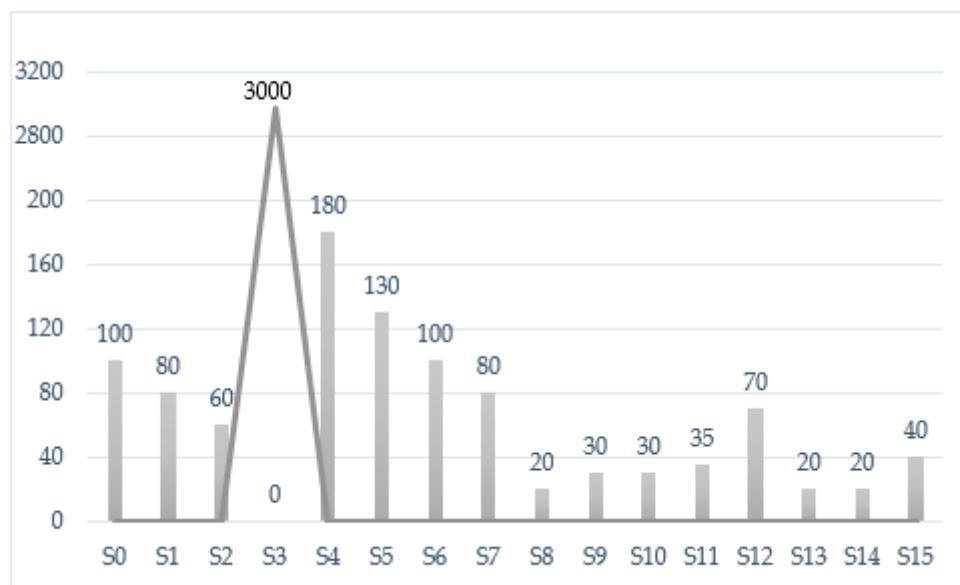


Figure 15. Electromagnetic wave power density for C<sub>3</sub> to S<sub>0</sub>, S<sub>1</sub>, . . . , and S<sub>15</sub>.

**Table 3.** Comparison of electromagnetic wave signal strength and total electromagnetic wave power density for  $S_0, S_1, \dots$ , and  $S_{15}$  to  $C_3$  and  $C_4$ .

Test Case 3				$C_3$		Test Case 4				$C_4$	
		Wi-Fi Analyzer		MROL				Wi-Fi Analyzer		MROL	
E.S.	Dist.	-dBm	Effect	-dBm	P. D.	E.S.	Dist.	-dBm	Effect	-dBm	P. D.
				$(10^{-6} \text{ W/m}^2)$						$(10^{-6} \text{ W/m}^2)$	
		m				m					
$S_0$	4	44	L	43	100	$S_0$	10	53	L	53	100
$S_1$	3.4	43	L	41	80	$S_1$	9	49	L	48	80
$S_2$	3.1	38	L	41	80	$S_2$	5	42	L	40	60
$S_3$	8.3	53	SD	51	60	$S_3$	0	35	L	35	3000
$S_4$	11	47	sd	47	200	$S_4$	19.3	52	sd	55	180
$S_5$	11.1	52	i	56	100	$S_5$	19.4	57	sd	54	130
$S_6$	0	35	L	33	3000	$S_6$	8.3	42	L	45	100
$S_7$	4	38	L	40	100	$S_7$	12.3	56	D	53	80
$S_8$	8	49	D	44	30	$S_8$	16.3	64	D	56	20
$S_9$	12	43	D	50	20	$S_9$	20.3	69	D	63	30
$S_{10}$	16	45	D	49	25	$S_{10}$	24.3	68	D	68	30
$S_{11}$	20	52	D	54	35	$S_{11}$	28.3	80	D	66	35
$S_{12}$	24	63	D	51	50	$S_{12}$	32.3	71	D	73	70
$S_{13}$	13.8	63	sd	55	20	$S_{13}$	5.5	43	sd	48	20
$S_{14}$	20.3	61	SD	56	20	$S_{14}$	12	55	D	41	20
$S_{15}$	24.3	60	si	71	30	$S_{15}$	16	64	SD	62	40
Total		786		782	3950	Total		900		860	3995

Considering electromagnetic wave power density, all embedded systems consumed  $3995 \times 10^{-6} \text{ W/m}^2$ ; measured results are illustrated in Figure 16. On the basis of all test case results, the third test case had better electromagnetic wave strength and less of an electromagnetic effect.

**Figure 16.** Electromagnetic wave power density for  $C_4$  to  $S_0, S_1, \dots$ , and  $S_{15}$ .

## 5. Conclusions

Embedded systems with smaller, cheaper, and easier-to-implement characteristics are more popular for designing smart objects, devices, applications, or services. Recently, there has been an increasing number of functions, such as wired, wireless, or/and sensor peripherals that are integrated into embedded systems to provide interconnected and collaborating services. As diverse embedded systems are continually set and joined up to smart offices, either electromagnetic wave power density or the communication strength is a significant issue considering energy-saving or cooperation work for all embedded systems. This work studied the layout of multiple embedded systems for communication

strength and electromagnetic wave power density optimization. Our prior works measured the original data of electromagnetic signal strength and power density for smart offices, shown in Figure 3. For the issue of electromagnetic signal strength, we analyzed deployment topology into an  $n$ -shaped layout and an  $n$ -shaped layout with a door in smart offices. In the  $n$ -shaped layout, we classified electromagnetic signal strength into local, direct, and semidirect effects, and their scope. Then, we defined a set of formulas to determine the effect of each embedded system. We presented local, direct, semidirect, indirect, and subindirect effects for an  $n$ -shaped layout with a door. Each effect was derived from the scope, and then defined a set of formulas. Those formulas can help users to quickly identify the scope of each effect while the communication center is set up. In the experiments, we measured each effect in either the  $n$ -shaped layout or the  $n$ -shaped layout with a door for four test cases. Experiment results indicated that the local effect had the best communication strength, but electromagnetic wave power density was critical. The direct effect had better communication strength and less consumption of electromagnetic wave power density than the semidirect effect did. By comparing the semidirect and indirect effects, the former generally had better communication strength than that of the latter. Regarding the subindirect effect, it consumed the least electromagnetic wave power density, but communication strength was the weakest among all effects. Lastly, a summary of the experiment results pointed to diverse effects with the optimization layout for embedded systems.

**Funding:** This research received no external funding.

**Acknowledgments:** The author would like to thank the Ministry of Science and Technology of the Republic of China, Taiwan, for financially supporting this research under Contract MOST 107-2221-E-143-003.

**Conflicts of Interest:** The author declares that there are no conflicts of interest regarding the publication of this paper.

## References

1. Fan, Y.-H. Energy-Efficient Clusters for Object Tracking Networks. *Energies* **2018**, *11*, 2015. [[CrossRef](#)]
2. Fan, Y.-H. Extensible Software Synthesis for Embedded Ubiquitous Learning Systems. *Adv. Electr. Comput. Eng.* **2015**, *15*, 133–140. [[CrossRef](#)]
3. Klemenjak, C.; Elmenreich, W. Yay—An open-hardware energy measurement system for feedback and appliance detection based on the arduino platform. In Proceedings of the 2017 13th Workshop on Intelligent Solutions in Embedded Systems (WISES), Hamburg, Germany, 12–13 June 2017; pp. 1–8.
4. Visutsak, P.; Daoudi, M. The smart home for the elderly: Perceptions, technologies and psychological accessibilities: The requirements analysis for the elderly in Thailand. In Proceedings of the 2017 XXVI International Conference on Information, Communication and Automation Technologies (ICAT), Sarajevo, Bosnia-Herzegovina, 26–28 October 2017; pp. 1–6.
5. Florea, I.; Rughinis, R.; Ruse, L.; Dragomir, D. Survey of Standardized Protocols for the Internet of Things. In Proceedings of the 2017 21st International Conference on Control Systems and Computer Science (CSCS), Bucharest, Romania, 29–31 May 2017; pp. 190–196.
6. Chen, L.; Cook, D.J.; Guo, B.; Chen, L.; Leister, W. Awareness in Cyber-Physical Human-Machine Systems. *IEEE Trans. Hum. Mach. Syst.* **2017**, *47*, 47. [[CrossRef](#)]
7. Bleda, A.L.; Luque, F.J.F.; Rosa, A.; Zapata, J.; Maestre, R. Smart Sensory Furniture Based on WSN for Ambient Assisted Living. *IEEE Sens. J.* **2017**, *17*, 5626–5636. [[CrossRef](#)]
8. Lalanda, P.; Gerber-Gaillard, E.; Chollet, S. Self-Aware Context in Smart Home Pervasive Platforms. In Proceedings of the 2017 IEEE International Conference on Autonomic Computing (ICAC), Columbus, OH, USA, 17–21 July 2017; pp. 119–124.
9. Adiono, T.; Tandiawan, B.; Fuada, S.; Muttaqin, R.; Fathany, M.Y.; Adijarto, W.; Harimurti, S. Prototyping design of IR remote controller for smart home applications. In Proceedings of the TENCON 2017—2017 IEEE Region 10 Conference, Penang, Malaysia, 5–8 November 2017; pp. 1304–1308.
10. Zeng, J.; Yang, L.T.; Ma, J.; Guo, M. HyperspaceFlow: A System-Level Design Methodology for Smart Space. *IEEE Trans. Emerg. Top. Comput.* **2015**, *4*, 568–583. [[CrossRef](#)]

11. Deuri, J.; Sathya, S.S. Cricket Chirping Algorithm for Multi-Objective Engineering Design Optimization. In Proceedings of the 2017 International Conference on Information, Communication and Embedded Systems (ICICES), Chennai, India, 23–24 February 2017; pp. 1–6.
12. Dutta, P.; Datta, D. Bi-level problem as a plain multi-objective optimization problem: A preliminary study. In Proceedings of the 2017 International Conference on Advances in Mechanical, Industrial, Automation and Management Systems (AMIAMS), Allahabad, India, 3–5 February 2017; pp. 69–73.
13. Zhou, Y. A Decomposition-Based Multi-Objective Tabu Search Algorithm for Tri-Objective Unconstrained Binary Quadratic Programming Problem. In Proceedings of the 22017 IEEE International Conference on Computational Science and Engineering (CSE) and IEEE International Conference on Embedded and Ubiquitous Computing (EUC), Guangzhou, China, 21–24 July 2017; Volume 1, pp. 101–107.
14. Wifi Analyzer Application, Download from Google Play Store of Mobile with Android Operating System. Available online: [https://play.google.com/store/apps/details?id=abdelrahman.wifianalyzerpro&hl=en\\_GB](https://play.google.com/store/apps/details?id=abdelrahman.wifianalyzerpro&hl=en_GB) (accessed on 7 April 2019).
15. Tenmars TM-196 Instrument. Available online: <https://www.testmeter.sg/products/Tenmars-TM-196-3-Axis-EMF-RF-Field-Strength-Meter-10MHz-to-8GHz/103> (accessed on 7 August 2019).
16. Arduino WeMos D1 Mini Platform. Available online: <https://escapequotes.net/esp8266-wemos-d1-mini-pins-and-diagram/> (accessed on 2 August 2019).
17. Fortinet FortiAP-221C. Available online: <https://www.cnet.com/products/fortinet-fortiap-221c-wireless-access-point-fap221ce/> (accessed on 7 August 2019).
18. Xiaomi ZMI Power Bank. Available online: <https://buy.mi.com/tw/item/3181500001> (accessed on 1 August 2019).



© 2020 by the author. Licensee MDPI, Basel, Switzerland. This article is an open access article distributed under the terms and conditions of the Creative Commons Attribution (CC BY) license (<http://creativecommons.org/licenses/by/4.0/>).